



## An Investigation of the Mechanical Property Behaviour of Copper/AA7075 Nanocomposites Based on Machine Learning

Raquel Virginia Colcha Ortiz<sup>1\*</sup>, María Albuja<sup>2</sup>, Eugenia Mercedes Naranjo Vargas<sup>2,3</sup>,  
Monica Alexandra Moreno Barriga<sup>2,3</sup>, Miguel Escobar<sup>2</sup>, Ximena Rashell Cazorla Vinuesa<sup>4</sup>,  
Jessica Paola Arcos Logroño<sup>4</sup>, Paul Montufar<sup>2</sup>, Paul Marcelo Tacle Humanante<sup>5</sup>

<sup>1</sup> Facultad de Ciencias Pecuarias, Escuela Superior Politécnica de Chimborazo (ESPOCH), Riobamba 060155, Ecuador

<sup>2</sup> Facultad de Ingeniería Mecánica, Escuela Superior Politécnica de Chimborazo (ESPOCH), Riobamba 060155, Ecuador

<sup>3</sup> Grupo de Investigación y Desarrollo de Nanotecnología, Materiales y Manufactura (GIDENM), Escuela Superior Politécnica de Chimborazo (ESPOCH), Riobamba 060155, Ecuador

<sup>4</sup> Sede Morona Santiago, Escuela Superior Politécnica de Chimborazo (ESPOCH), Riobamba 060155, Ecuador

<sup>5</sup> Facultad de Recursos Naturales, Escuela Superior Politécnica de Chimborazo (ESPOCH), Riobamba 060155, Ecuador

Corresponding Author Email: [raquel.colcha@esepoch.edu.ec](mailto:raquel.colcha@esepoch.edu.ec)

Copyright: ©2024 The authors. This article is published by IETA and is licensed under the CC BY 4.0 license (<http://creativecommons.org/licenses/by/4.0/>).

<https://doi.org/10.18280/mmep.110807>

### ABSTRACT

**Received:** 2 April 2024

**Revised:** 29 June 2024

**Accepted:** 5 July 2024

**Available online:** 28 August 2024

#### Keywords:

*copper, AA7075, mechanical properties, machine learning, support vector regression, Puk kernel*

Predicting the mechanical characteristics of Copper (Cu) -AA7075 nanocomposites produced by the powder metallurgy (PM) method was investigated using a machine-learning (ML) strategy to speed up production and characterization while offering physical insights into the properties of the materials. To build prediction models, six methods are used, including chemical arrangement and the porosity of the composites serving as the defining characteristics. The outcome indicates that the Sequential minimum optimization support vector regression Puk kernel (SMO reg/Puk) model produced the most precise predictions. Indeed, among the six models, its forecasts had the maximum correlation coefficient (CC) and the slightest inaccuracy. Using the SMO reg/Puk model, authors could make predictions about the tensile strength (TS) and hardness (HB) of Cu-AA7075, and this information guided the composition design efforts. The desired chemical composition, including a porosity of around 12.3%, a tensile strength of more than 360 MPa, and hardness of HB (140-145), was achieved in a Cu with 14 wt% Al and 7 wt% Ni nanocomposites. Cu-14Al-7Ni nanocomposites with the targeted tensile strength (394 MPa) and hardness (HB 143) was developed using the SMO reg/Puk model as a roadmap.

## 1. INTRODUCTION

The high strength, hardness, wear resistance, and corrosion resistance [1, 2], copper alloys find widespread application in various applications, including pumps, bearings, propellers, engineering tools, dies, etc. [3, 4]. Its tensile strength and hardness best exemplify aluminium bronze's mechanical qualities [5, 6]. It is currently necessary to use destructive testing procedures that are both time-consuming and expensive to evaluate aluminium bronze's mechanical properties [7, 8]. Because of this, there is a pressing need for a reliable way of estimating aluminium bronze's mechanical qualities [9].

It has become increasingly common in recent years to employ machine learning methods to forecast the mechanical properties of materials [10]. The bending toughness and hardness of AMC could be accurately predicted using the back-propagation artificial neural network (BP-ANN) model developed by Pandya et al. [11] and Li et al. [12]. The researcher made predictions of Aluminium-Copper-Magnesium-Silver alloy strength using support vector

regression (SVR) [13]. This study demonstrated that the SVR model outperformed BP-ANN under identical training conditions [14, 15]. Niobium-Silicon alloy's UTS was predicted using a high-precision ANN model created by Shi et al. [16], Taşgın and Ergin [17]. They used the model to help them achieve their goal of increasing the sample's strength by altering its microstructure. To forecast the mechanical properties of A357 alloy, Hua et al. [18] and Kazemi-Navaei et al. [19] used an ANN model, and their findings indicate that the Back Propagation model was highly accurate. Supraja Reddy and Ram Gopal Reddy [20] used the Artificial Neural network model to forecast the HB of 18-5PH and optimize a temperature treatment procedure to attain the highest possible HB [21].

This study addresses a significant advance in the field of materials science and engineering by introducing a novel approach to predicting the mechanical properties of Cu-AA7075 nanocomposites using machine learning (ML) algorithms.

In the present research, a large dataset, including a comprehensive collection of 142 experimental tensile strength

data and 100 hardness data, is analysed to accurately model and predict the TS and HB of Cu-AA707 nanocomposites, exploiting the chemical composition and porosity of these composites as key characteristics, addressing the lack of predictive models in the existing literature and providing a data-driven basis for predicting the mechanical properties of copper alloys. This unprecedented data collection, which combines results from current laboratory experiments with data drawn from a wide range of publications, enables the development of much more refined and accurate predictive models than those available in previous studies. Six different ML algorithms were employed, including sophisticated models such as the Sequential Minimum Optimisation (SMO) algorithm for Support Vector Regression (SVR) with both normalised Poly Kernel and Puk kernel, the study demonstrates a versatile and nuanced approach to predictive modelling. This diverse application of multiple algorithms is a novel approach in the field of predicting the mechanical properties of Cu-AA7075 nanocomposites, which serves to identify the SMO algorithm for SVR with a Puk kernel as particularly effective.

## 2. METHODS AND MATERIALS

Six different machine learning (ML) models were used for predicting the tensile strength (TS) and hardness (HB) of Cu-AA7075 nanocomposites, providing a rationale for their selection based on the unique advantages and inherent limitations of each approach. The models selected include Sequential Minimum Optimization (SMO) algorithm for Support Vector Regression (SVR) with normalized Poly Kernel and Puk kernel, Standard Linear Regression (LR), Multilayer Perceptron (MLP), and SVR with poly kernel.

### 2.1 Justification for model choice

Sequential Minimum Optimization (SMO) for SVR with Puk kernel: Chosen for its efficient handling of non-linear data and its ability to produce high-quality predictions in cases where relationships between variables are complex. This model showed the best performance among all evaluated models, reflecting its superior capability in generalization and dealing with high-dimensional data spaces. The advantage of using the Puk kernel over traditional kernels lies in its flexibility and adaptability to the specifics of the dataset, potentially resulting in better prediction accuracy.

SMO for SVR with normalized Poly Kernel: This variant of SVM is designed to manage the non-linearity of data by mapping the input features into a higher-dimensional space using a polynomial kernel. It's known for high accuracy in certain applications, although its performance can be sensitive to the choice of parameters and the scaling of input data.

Standard Linear Regression (LR): A basic yet powerful model for understanding relationships between variables. Its inclusion allows for evaluating the potential linear association between the compositional and process variables with the mechanical properties of the nanocomposites. While it's less capable of capturing complex non-linear patterns, it provides a benchmark for comparison and is computationally less intensive.

Multilayer Perceptron (MLP): This neural network model is included for its strong capacity in approximating non-linear functions and interactions among variables. MLP can capture

intricate patterns in the data through its layer(s) and neuron connections but requires careful tuning of its architecture and parameters to avoid overfitting.

SVR with poly kernel: Similar to the SMO-reg variants, this model leverages the polynomial kernel for tackling non-linear relationships but is differentiated by its implementation through a different optimization approach. SVR models are particularly valued for their robustness and efficiency in handling high-dimensional spaces.

SMO algorithm for SVR with Poly Kernel: This choice capitalizes on the optimization efficiency of the SMO algorithm, combined with the versatility of the poly kernel in modeling non-linear relationships. This combination aims to strike a balance between computational efficiency and predictive capability.

### 2.2 Advantages and limitations

*Advantages:* The diverse selection of models facilitates a comprehensive exploration of the data, allowing the study to capture a wide range of underlying patterns and relationships. From simple linear associations to complex non-linear behaviors, the chosen models offer a spectrum of computational techniques to best approximate the mechanical properties of Cu-AA7075 nanocomposites based on its chemical composition and process parameters.

*Limitations:* While these models encompass a broad set of ML techniques, each comes with its considerations. For instance, SVM-based models (including SMO variations) can be computationally intensive and sensitive to parameter tuning. Conversely, linear regression, though less complex, might not capture all non-linear interactions within the data effectively. MLPs, while powerful, require extensive data for training to achieve generalization without overfitting.

The distinction in model selection is meant to harness the strengths of each method while acknowledging their limitations, aiming to provide a balanced and comprehensive approach to predicting the mechanical properties of Cu-AA7075 nanocomposites. Through their comparative analysis, the study seeks not only to identify the most accurate model but also to deepen the understanding of how different ML techniques interpret and learn from materials science data.

### 2.3 Modeling process

The three phases of constructing an ML model are Collecting data, modeling development, and Authentication of the model.

#### 2.3.1 Collecting data

Three limitations were placed on the data collection process regarding the chemical components and processing technique.

- First, the other alloying elements can't make up a more significant percentage of their total mass than Al does.
- Cu-AA7075 nanocomposites were only prepared through casting and PM to limit the impact of process on material characteristics.
- Third, only traditional alloying elements like Aluminium, Iron, Nickel, and Manganese were used because there was a shortage of data for additional features, which could have impacted the reliability of the data withdrawal.

The microstructure and characteristics of composites are primarily determined by its chemical composition [22, 23]. The chemical compositions are Silicon 0.08%, Iron 0.24%,

Copper 1.5%, Manganese 0.06%, Magnesium 2.4% Chromium 0.2%, Zinc 5.8% and balance aluminium. The percentage of aluminium in Cu-AA7075nanocomposites varies from 6% by weight to 15%, making aluminium a crucial alloying element. Only the phase is present for nanocomposites with Al contents below 9.5 wt%, resulting in low hardness and strength. When the percentage of Al in an alloy rises over 9.5 wt%, a mixture of the phase and the 2 phase forms, leading to increased hardness but diminished strength. The structure and qualities of an alloy can be modified by adding other alloying elements like Nickel, Iron, or Manganese [24]. The addition of iron can refine grains and enhance mechanical characteristics [25]. In contrast, the addition of nickel can expand the  $\alpha$ -phase zone and grain refinement, and the addition of manganese can lower the conversion temperature [26].

The porous of sintered composite significantly affects its characteristics. As porosity increases, TS decreases; ductileness and abrasive resistance are very vulnerable to pore formation [27, 28]. Unlike sintered compacts, the penetrability of molding alloys is not nil. Consequently, porosity is also employed to distinguish between the two methods.

The percentages of aluminium, Iron, Nickel, and Manganese by weight and the material's porosity were used to characterize the material in this investigation [29].

A total of 142 items of experimental data on tensile strength (TS) and 100 things of experimented data on hardness were gathered after the restrictions and descriptors were applied. Both current study laboratory experiments and previous studies' results from the literature [30-32] were used to compile the datasets.

### 2.3.2 Modeling

Data mining has seen the widespread application of neural networks and support vector machines (SVMs) [33]. The mathematical technique known as a neural network is nonlinear and can adapt to new data. It has proven adept at making predictions where precise descriptions are hard to get from numerical models [34]. However, under finite sample settings, an SVM's great generalization capacity allows it to handle the challenge of high-dimensional data model creation [35].

To construct a prediction, model six machine learning algorithms were used. They are:

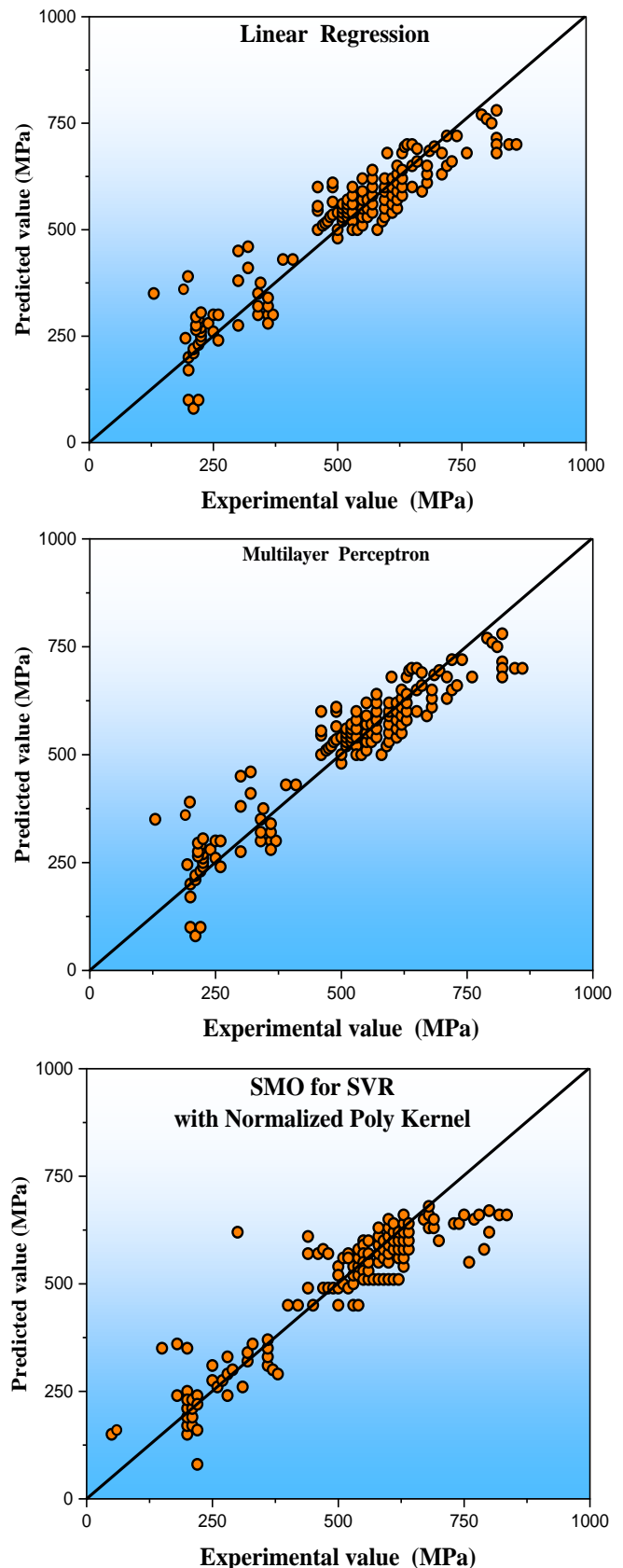
- Sequential Minimum Optimization (SMO) algorithm for SVR normalized Poly Kernel (SMOreg/ norpoly)
- Standard linear regression (LR)
- Multilayer perceptron (MLP)
- SVR with poly kernel (SVR/poly)
- SMO reg/Puk (sequential minimum optimization (SMO) algorithm for SVR (SMOreg) Puk kernel)
- SMO algorithm for SVR with poly kernel (SMO reg/poly)

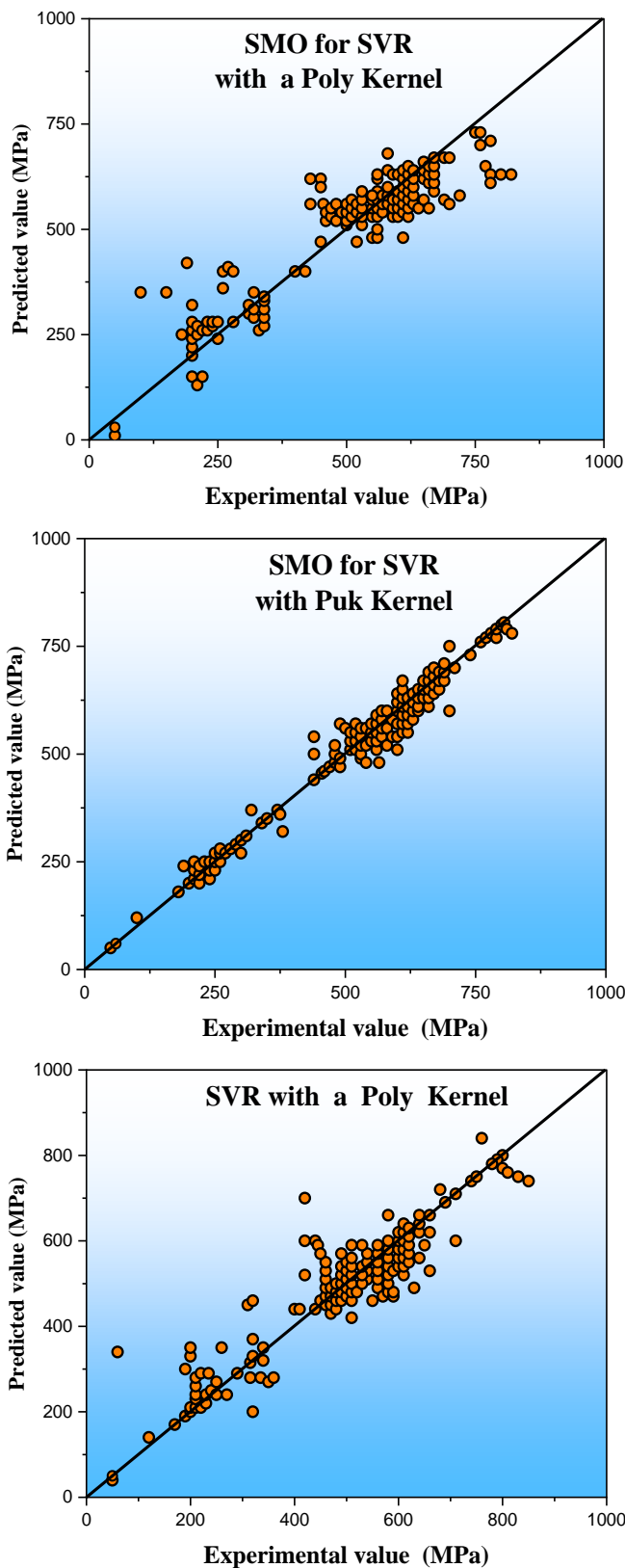
Five rounds of cross-validation were performed for this paper. A total of five roughly equal parts of the dataset were extracted. The authors [36] utilized each subset once for testing purposes. It was decided that the other four parts would serve as training data whenever one part of the data represented the testing data [37]. The data presented here are the mean values from five separate tests.

Figures 1 and 2 display the expected TS and HB range against the corresponding experiment results. The mechanical characteristics of the nanocomposites are accurately predicted by the model, as both the experimental and anticipated values

are roughly on the line  $Y=X$ . The SMO algorithm for SVR with a Puk kernel model had the most refined fit throughout training, as seen in Figures 1 and 2.

The accuracy of the forecast models developed using the six algorithms was measured using the correlation coefficient (CC), the mean absolute error (MAE), and the root-mean-squared error (RMSE) [38, 39].

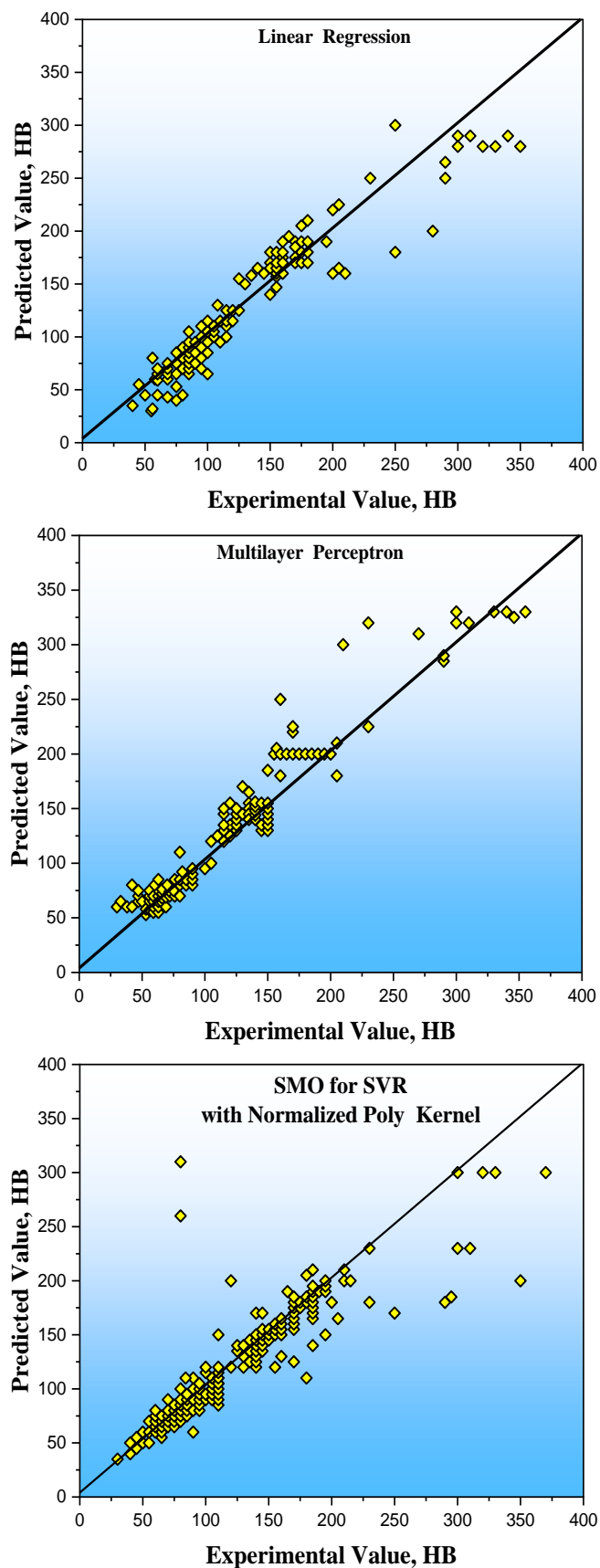




**Figure 1.** Evaluation of tensile strength prediction value using six ML algorithms on a training dataset

The values of the correlation coefficient, the root-mean-squared error, and the mean absolute error for the six ML models are shown in Figure 3. The best performance is demonstrated by the SMO algorithm for the SVR Puk kernel, with CC values of 0.9215 and 0.9416 for the TS model and the HB model respectively. Tensile strength predictions from the SMO algorithm for the SVR Puk kernel model have a mean

absolute error (MAE) of 53.2486 MPa, and a root means square error (RMSE) of 74.7712 MPa, whereas SMOreg/Puk model hardness predictions have a MAE of HB 17.9264 and an RMSE of HB 27.2981. These numbers are less than predicted by competing models. Because of this, the Sequential minimum optimization SVR Puk model was chosen to estimate the material hardness and tensile strength.



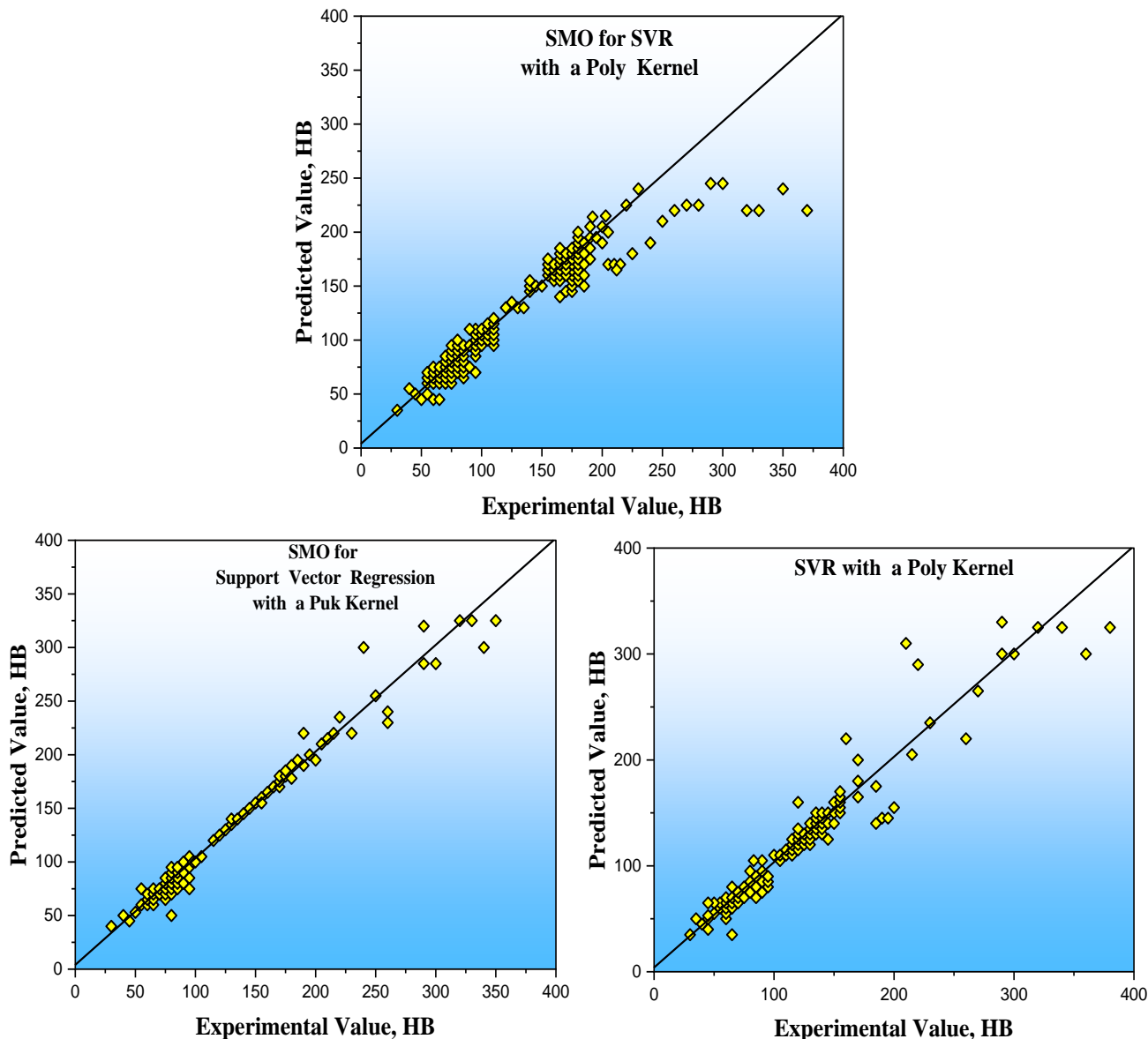


Figure 2. Evaluation of Hardness prediction value using six machine learning algorithms on a training dataset

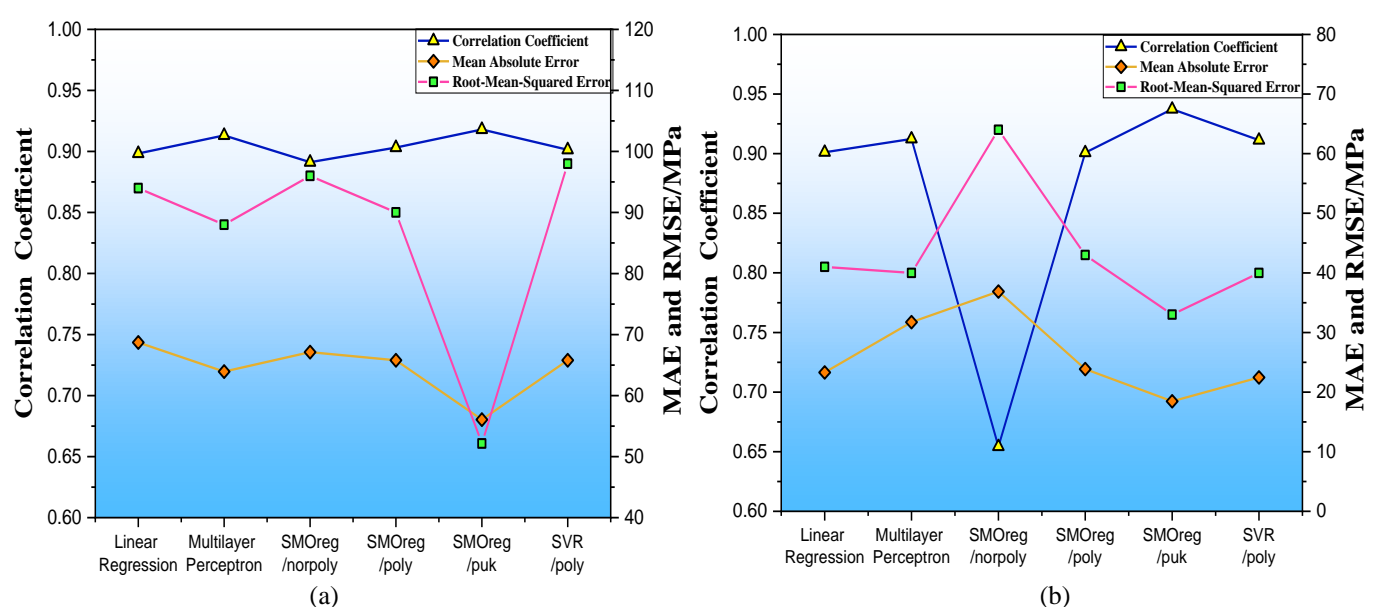
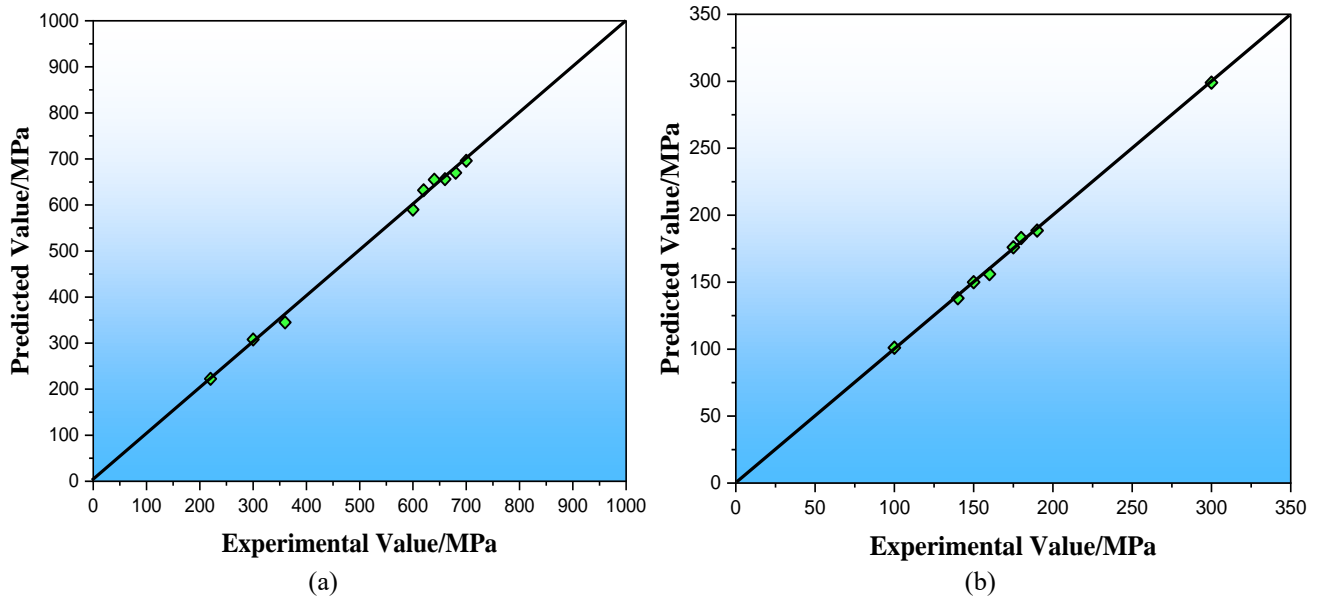


Figure 3. Correlation coefficient, Root Mean Square Error, and Mean Absolute Error of six ML models functional to the data of training: (a) Tensile Strength (TS); (b) Hardness (HB)



**Figure 4.** SMO algorithm for SVR Puk kernel model predictions for (a) TS and (b) HB on the authentication dataset related to the equivalent experimented results

### 2.3.3 Authentication of model

Researchers validated the SMO reg/Puk prediction model by comparing its predictions of tensile strength and hardness to experimental values from evaluation data (Figure 4). Authentication datasets were gathered from several sources, including tests and scholarly researchers [40-43], in addition

to the training dataset. The lists of validation datasets can be found in Table 1. Validation dataset predictions for TS and HB are consistent with experimental results. The highest deviation in TS is only 31.52 MPa (Figure 4(a)), while the maximal deviation is only HB 9.1 (Figure 4(b)).

**Table 1.** Model authentication data for the SMO algorithm SVR Puk kernel forecast

S. No.	Aluminum/wt%	Nickel/wt%	Iron/wt%	Manganese/wt%	Porosity/%	TS/MPa	Hardness/HB	References
1	10.31	5.50	4.94	1.20	0.00	697.00	178.00	[44]
2	10.42	6.96	5.09	1.21	0.00	657.00	-	[44]
3	10.66	8.94	5.05	1.21	0.00	592.00	184.00	[44]
4	11.5	6.00	5.60	1.00	0.00	645.00	-	Current project
5	12.0	5.70	5.20	1.28	0.00	654.00	189.60	Current project
6	12.4	5.31	5.33	3.05	0.00	634.00	-	[45]
7	13.2	0.00	5.10	0.00	12.4	309.00	157.00	Current project
8	14.0	0.00	0.00	5.00	11.80	351.00	160.00	Current project
9	11.10	5.30	5.00	0.00	13.04	223.60	102.00	Current project
10	9.84	0.00	0.91	0.00	0.00	-	138.00	[46]
11	14.10	0.35	4.00	1.25	0.00	-	299.00	[47]
12	12.20	6.00	6.00	0.00	11.55	-	138.00	Current project

### 2.4 Model application

The Cu-AA7075 composition was designed with the SMO algorithm for the SVR Puk kernel model to ensure the desired mechanical qualities would be achieved. This compositional study aimed to develop a novel high-strength Cu-AA7075 composite with a porous of around 12.3%, a tensile strength of more than 360 MPa, and hardness of HB 140-145. With its high strength and excellent self-lubricating properties, the Cu-AA7075 nanocomposites is ideal for use as a bearing material. The structure's pores accommodate either a solid lubricant like graphite or MoS<sub>2</sub> or a liquid lubricant like lubricating oil.

Figure 5 and Figure 6 illustrate a distribution map of the TS and HB with the change of each descriptor, based on the values forecast employing the SMO algorithm SVR Puk kernel algorithm for the Cu-AA7075. As can be shown in Figure 5, the Cu-AA7075 nanocomposites reaches a tensile strength of 360 MPa when the porosity is 12.3%. The TS of the

nanocomposite is maximized between 11.5 and 12.0 wt% aluminium. The TS of the nanocomposite is maximized between 6.6 and 7.1 wt% Nickel. A nanocomposite strength generally improves as manganese concentration increases from 0% to 3.3-3.8 wt%. However, as Iron content rises, tensile strength falls.

As shown in Figure 6, the desired level of nanocomposite hardness is achieved when the porosity is less than 13.0%. The hardness of the nanocomposite rises linearly with the amount of aluminium present [48]. The desired level of alloy hardness is achieved at an aluminium concentration of more than 14.1%. The hardness drops as the Ni or Mn content rises. For the desired hardness level in a nanocomposite, the Ni concentration must be less than 7.2 wt%. All of the nanocomposites may achieve the desired hardness within the range of the measured Mn concentration [49]. Hardness, however, increases with Fe content before decreasing again. The nanocomposite can achieve the desired hardness if the Fe

percentage is below 4.1wt percent. In this situation, the element content range chosen for hardness also encompasses the element content range selected for TS.

TS and HB were estimated by employing the Sequential minimum optimization support vector regression Puk kernel model for the following composition ranges based on the findings above: Cu-(13.6-14.1)Al, Cu-(13.6-14.1)Al-(6.6-7.1)Ni, Cu-(13.6-14.1)Al-(6.6-7.1)Ni-(3.3-3.8)Mn, and Cu-(13.6-14.1)Al-(3.3-3.8)Mn are all examples of alloys with these percentages of Al, Ni, Fe, and Mn. Changes in chemical will occur in 0.1 wt% increments. The mechanical characteristics of the nanocomposite, such as its TS and HB, were found to achieve target values upon the study of the prediction findings when the chemical composition was near to Copper-14Al-7Ni.

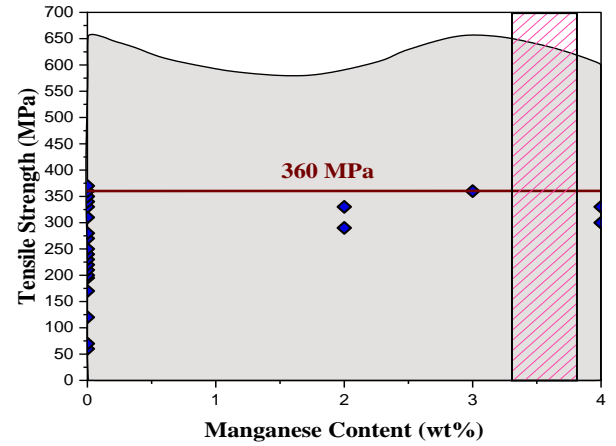
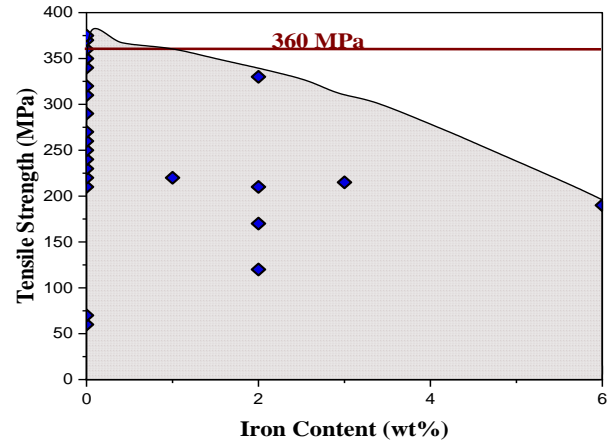
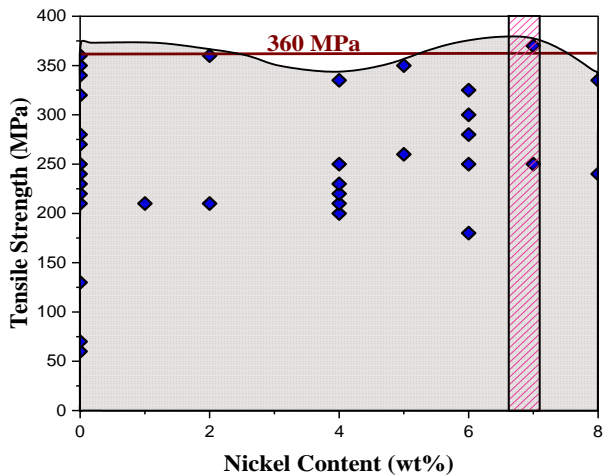
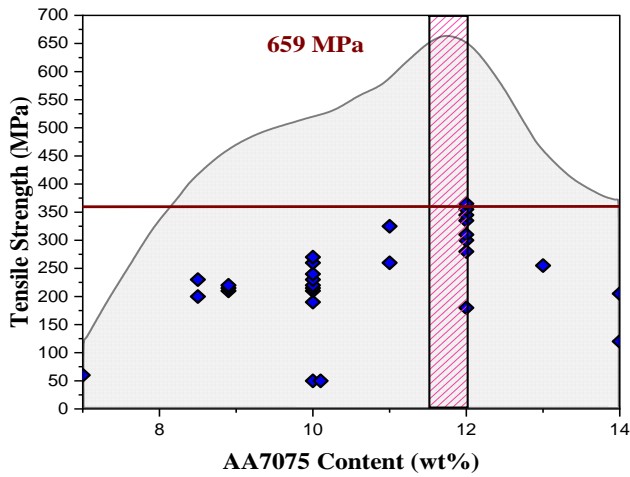
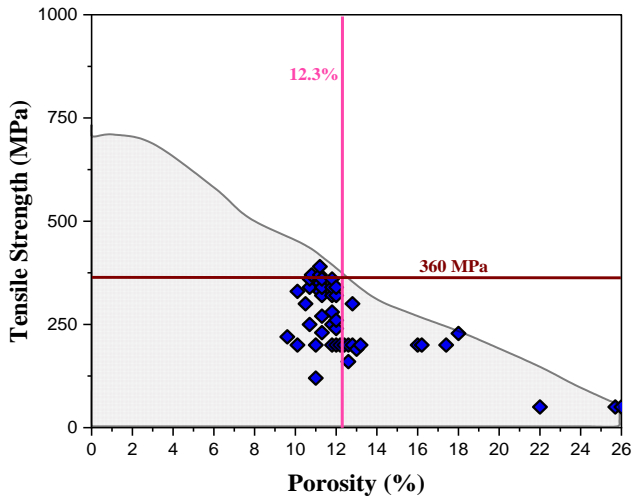
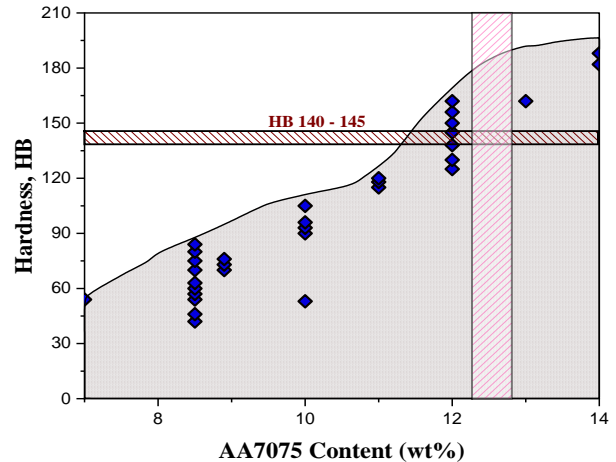
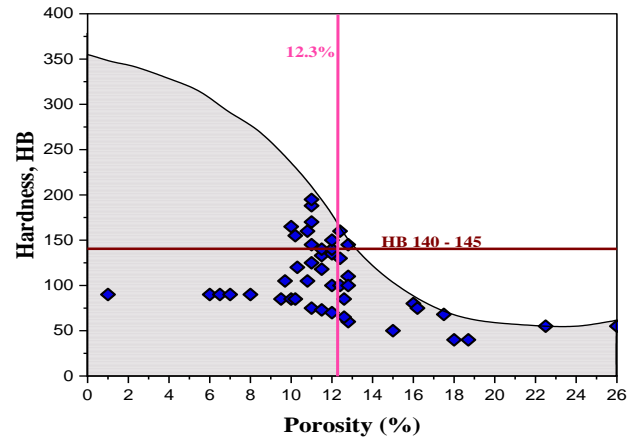
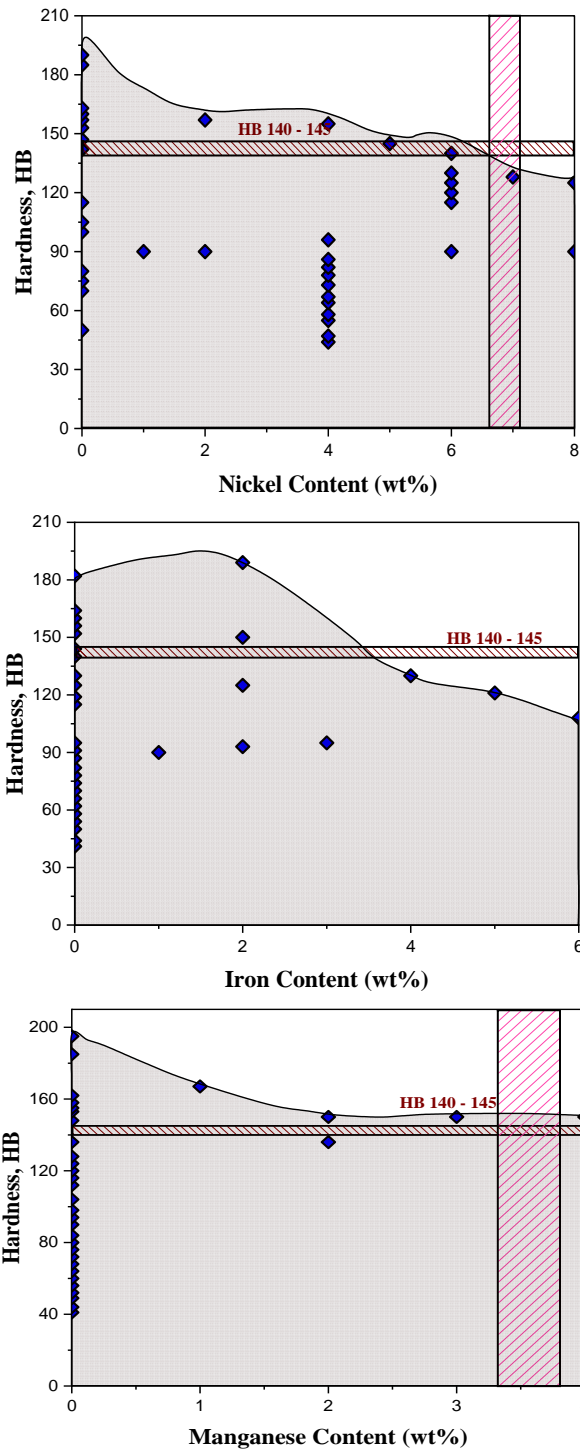


Figure 5. SMOreg/Puk model-obtained tensile strength distribution of the nanocomposite as a function of porosity and composition





**Figure 6.** SMOreg/Puk model-obtained hardness distribution of the nanocomposite as a function of porosity and composition

### 2.5 Experimental methods

From a review of the available literature [50, 51], the authors settled on a target porosity of 12.3% for the Cu-AA7075 nanocomposites and determined the following process parameters for its fabrication. The raw materials were the powdered elements copper, aluminum, and nickel. There are three separate numbers in Table 2 labelled "D15," "D55," and "D95" that correspond to the particle size distribution's cumulative mass at the locations where it reaches 15%, 55%, and 95% from the small-particle-diameter side, respectively. Three hours were spent in a tube mixer combining Cu powder

with 14 wt% Al and 7 wt% Ni. At 550 MPa, discs of the blended powder measuring 20 mm in diameter were compacted. The green compact was heated in an H<sub>2</sub> environment to 1000°C for 1 hour at a heating rate of 5°C/min in a furnace.

**Table 2.** Features of the experimented powders

Powders	Particle-Size Distribution (µm)			Purity (wt%)	Method of Manufacture
	D15	D55	D95		
Copper	13.1	24.2	43.6	99.9	Electrolytic
Nickel	5.6	13.2	29.4	99.8	Carbonylation method
Aluminum	11.2	18.2	29.3	99.7	Argonatomized

An optical microscope (RX50M) and a scanning electron microscope (JSM-7001F) were used to examine the materials' microscopic structure, before SEM analysis the specimen was subjected to polishing using emery sheet. Energy-dispersive spectroscopy (EDS) was used on a scanning electron microscope (SEM) to explore the elemental distributions. The samples were analyzed by X-ray diffraction (XRD) with the help of a diffractometer. Hardness was assessed with a Brinell sclerometer (model HB3000), and TS was evaluated with an Instron 5569 UTM equipment.

Using Archimedes' equation, authors determined the compacts' sintered density, ( $\rho_s$ ) and the authors determined the specimen's porosity ( $\varepsilon$ ) using the subsequent Eqs. (1) and (2):

$$\rho_a = 1/(x_1/\rho_1 + x_2/\rho_2 + \dots + x_n/\rho_n) \quad (1)$$

$$\varepsilon = 1 - \rho_s/\rho_a \quad (2)$$

where,  $\rho_a$ : theoretic density;  $\rho_n$ : the density of  $n$ th element;  $x_n$ : mass of  $n$ th element.

### 3. RESULTS AND DISCUSSIONS

The significance of the MAE and RMSE as shown in Figure 7 values lies in their capacity to quantify the average magnitude of the errors in predictions made by the machine learning models, without considering their direction. The MAE gives a straightforward measure of prediction error magnitude, while RMSE gives a sense of the prediction error in the same units as the original measurements, with more weight to larger errors due to its quadratic scoring.

For the tensile strength (TS) predictions, the SMO algorithm for the SVR with a Puk kernel demonstrated the lowest MAE of 53.2486 MPa and RMSE of 74.7712 MPa. This indicates not just a tighter clustering of predicted values around the actual values but also fewer and less significant outliers in predictions as compared to other models. Similarly, for the hardness (HB) predictions, the SMOreg/PUK model achieved an MAE of 17.9264 and an RMSE of 27.2981, underscoring its superior prediction accuracy and consistency relative to competing models.

Figure 8 shows optical micrographic image of the copper-14Al-7Ni alloy. All the alloys had a microstructure that included a -Cu matrix phase (the yellowish areas), a NiAl phase (the brownish regions), and an Al<sub>4</sub>Cu<sub>9</sub> phase (the gray areas), as well as many pores. Figure 9 shows the Scanning Electron Microscope image of Cu-14Al-7Ni and Table 3 illustrates the EDS phase analysis results broken down by

element. At the interface among the -Cu phase and the Al<sub>4</sub>Cu<sub>9</sub> phase, as well as within the -Cu phase, a large no of granular Nickel-Aluminium phases precipitated. In contrast, the Al<sub>4</sub>Cu<sub>9</sub> stage exhibited an uneven morphology. In Figure 10, the X-ray Diffraction pattern of the nanocomposite correlates well with the EDS analysis results.

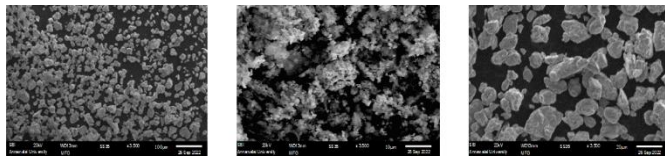


Figure 7. SEM images of powders: (a) Copper, (b) Aluminium and (c) Nickel

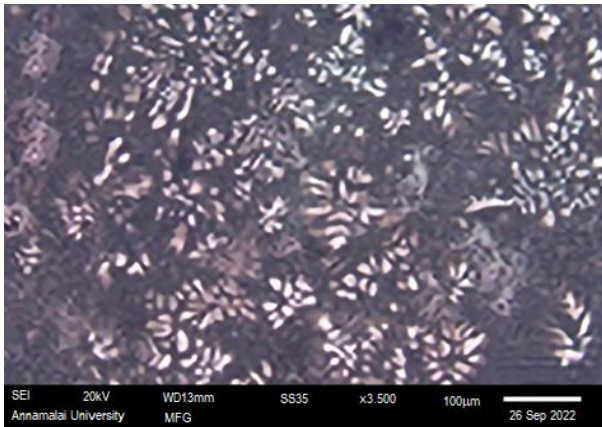


Figure 8. Optical image of the Copper-14Al-7Ni nanocomposite

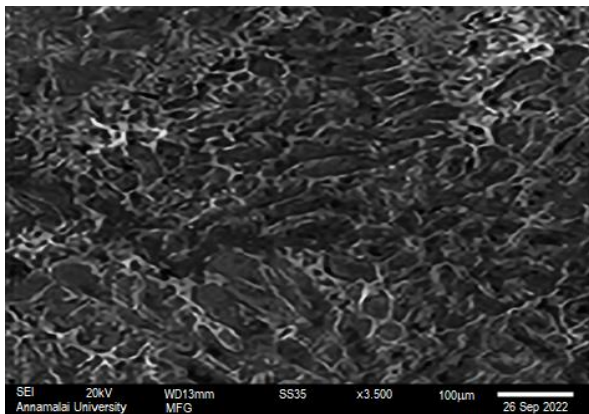


Figure 9. Scanning electron microscopic image of the Copper-14Al-7Ni nanocomposite

Table 3. An EDS study of the Cu-14Al-7Ni nanocomposite various phases

Phase	Copper (Cu)	Aluminum (Al)	Nickel (Ni)
α-Cu	79.81	19.26	1.33
Ni-Al	13.26	46.63	42.51
Al <sub>4</sub> Cu <sub>9</sub>	62.33	33.41	6.62

Based on the published literature, the Cu-14Al-7Ni vertical section was depicted and shown in Figure 11 [52]. On cooling, the -Cu phase first formed near the boundary of -AlCu<sub>3</sub>. This eutectoid reaction happened when the temperature dropped to the eutectoid reaction temperature for -AlCu<sub>3</sub>-Cu + NiAl. The

distribution of the NiAl phase at the grain boundaries of the copper phase efficiently stymied the development of the copper phase. The second eutectoid reaction (-AlCu<sub>3</sub>-Cu + NiAl + Al<sub>4</sub>Cu<sub>9</sub>) occurred at around 510°C. Since the -AlCu<sub>3</sub> stage was depleted during the first eutectoid reaction, the Al<sub>4</sub>Cu<sub>9</sub> phase fraction was significantly reduced by the smaller number of products formed during the second eutectoid reaction. Due to the delayed furnace cooling procedure, martensite was not found in the present investigation.

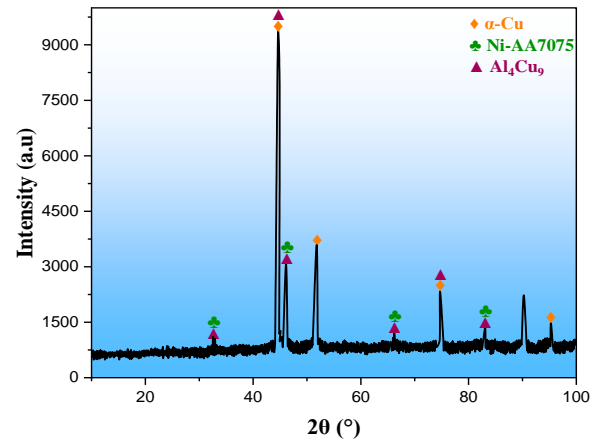


Figure 10. X-ray diffraction pattern of the Copper-14Al-7Ni nanocomposite

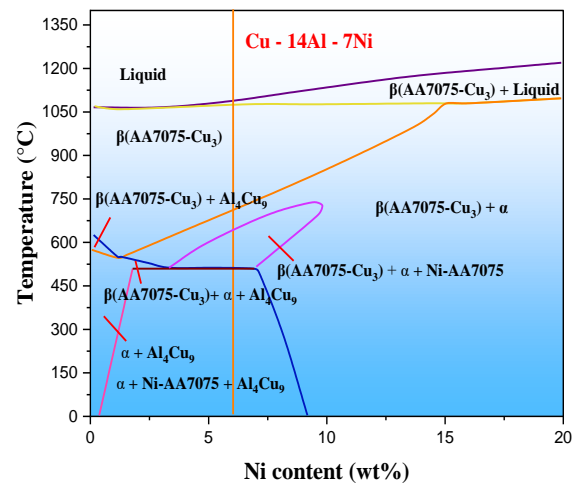


Figure 11. Vertical section of Cu-14Al-xNi [49]

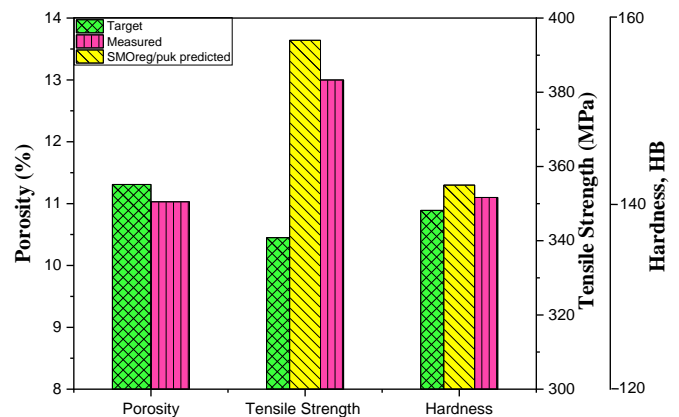


Figure 12. Cu-14Al-7Ni nanocomposite hardness, tensile strength, and porosity

Figure 12 summarizes the nanocomposite permeability, tensile strength, and hardness. The sintered samples had a porosity of 11.31%, which is 0.28% lower than the design goal. About 394 MPa is the tensile strength, which is 40 MPa higher than the target value and 10 MPa more elevated than the SMOreg/Puk model anticipated. The SMOreg/Puk model predicted a value of HB 142 for the hardness. However, the actual value is HB 143. That's why the authors saw an agreement between predicted and observed values in the experiments. Due to the nanocomposite's improved -Cu phase, fine-grain reinforcement was achieved. In addition, the strength of the nanocomposite was enhanced by the presence of several granular NiAl phases.

All of this evidence suggests that the SMO reg/Puk model is a valuable tool for predicting the characteristics of Cu-AA7075 nanocomposites and designing their chemical make-up. The SMO algorithm is commonly employed to predict the mechanical aspects of structural materials due to its fast training and good generalization performance [53]. The Puk kernel's superior mapping capabilities mean it excels at solving a wide range of mapping challenges. The SMO algorithm's generalization performance can be enhanced by the Puk kernel.

### 3.1 Comparison between measured and SMOreg/Puk-predicted values

The optimized composition of the Cu-AA7075 nanocomposite, aimed at achieving a tensile strength of more than 360 MPa and a hardness of 140-145 HB, was experimentally achieved with an actual composition close to Copper-14Al-7Ni. The experimental results exhibited a tensile strength of 394 MPa and a hardness of 143 HB. According to the SMOreg/Puk model predictions, for this composition, the tensile strength and hardness were anticipated to be in the proximity of 390 MPa and 140 HB, respectively.

### 3.2 Results-based implementation

The achieved tensile strength (TS) of 394 MPa and hardness (HB) of 143 for the developed Cu-14Al-7Ni nanocomposites represent noteworthy achievements when comparing these properties to those of common bearing materials. Traditional bearing materials, such as 52100 bearing steel, exhibit higher hardness (approximately 700 HB) and tensile strength (around 860-1200 MPa) due to their fully martensitic microstructure following heat treatment. Bronze bearings, on the other hand, show lower TS and HB, with values around 276 MPa for tensile strength and 60-100 HB for hardness, which highlights the Cu-14Al-7Ni composite's competitive placement in the spectrum of bearing material properties. It provides a balanced blend of strength and wear resistance, positioning it as a potential candidate for applications where traditional materials either exceed necessary specifications or fail to meet specific requirements.

## 4. CONCLUSIONS

This research provides an in-depth insight into the relationship between the chemical composition, porosity and mechanical properties of Cu-AA7075 nanocomposites. It expands current knowledge on how alloying elements such as aluminium, nickel, iron and manganese, as well as porosity,

affect tensile strength and toughness, offering valuable guidelines for future alloy development.

This research introduces new methodologies and analytical frameworks that significantly improve the predictability and understanding of the mechanical properties of Cu-AA7075 nanocomposites. It extends the application of machine learning algorithms beyond theoretical exploration, providing practical insights and tools for materials scientists and engineers to design materials with optimal properties.

Machine learning was employed in this study to make predictions about the TS and HB of Cu-AA7075 nanocomposite and to suggest how best to design their compositions to attain these targets. Chemical arrangement and porosity were used as the primary defining characteristics for the six algorithms employed to build the prediction models. This study's datasets were culled from several experiments and published studies. Here is a quick rundown of the key findings:

- SMO reg/Puk model had the highest accuracy rate out of the six models tested. It was the most accurate and showed the strongest correlation. TS and HB errors in the sequential minimum optimization algorithm SVR Puk model are lesser than 31.52 MPa and 9.1 HB, correspondingly, which is in good agreement with the experimental data.

- The desired chemical composition, including a porosity of around 12.3%, the tensile strength of more than 360 MPa, and hardness of HB (140-145), was achieved in a Cu with 14 wt% Al and 7 wt% Ni nanocomposites. After that, the powder metallurgy method was employed to manufacture the nanocomposite, which yielded desirable results in terms of TS (394 MPa), hardness (HB 143), and porosity (11.31%).

The study achieves a breakthrough in predictive accuracy, evidenced by the high correlation coefficients (CC) of 0.9215 for tensile strength and 0.9416 for hardness predictions using the SMO algorithm for SVR with a Puk kernel. These levels of accuracy surpass those reported in previous studies, marking a significant step forward in the reliable prediction of material properties.

Future studies could explore a broader range of compositions and include additional alloying elements to further enhance the material properties of Cu-AA7075 nanocomposites. Integrating machine learning predictions with detailed thermodynamic modeling could provide deeper insights into the phase transformations and their impact on properties.

Future studies could explore the relationship between processing conditions (e.g., sintering temperature, pressure, and time) and the mechanical properties of the nanocomposites could yield novel insights into optimizing manufacturing procedures for enhanced material performance.

Future studies could examine the environmental impact and sustainability of the production process for Cu-AA7075 nanocomposites, including the lifecycle assessment from raw material procurement to product end-of-life, could provide a pathway towards greener manufacturing practices.

## REFERENCES

- [1] López-Martín, C. (2021). Effort prediction for the software project construction phase. *Journal of Software: Evolution and Process*, 33(7): e2365. <https://doi.org/10.1002/smr.2365>
- [2] Deng, Z.H., Yin, H.Q., Jiang, X., Zhang, C., Zhang, G.F., Xu, B., Yang, G., Zhang, T., Wu, M., Qu, X.H. (2020).

- Machine-learning-assisted prediction of the mechanical properties of Cu-Al alloy. *International Journal of Minerals, Metallurgy and Materials*, 27: 362-373. <https://doi.org/10.1007/s12613-019-1894-6>
- [3] Kar, S., Pathakoti, K., Tchounwou, P.B., Leszczynska, D., Leszczynski, J. (2021). Evaluating the cytotoxicity of a large pool of metal oxide nanoparticles to *Escherichia coli*: Mechanistic understanding through in vitro and in silico studies. *Chemosphere*, 264: 128428. <https://doi.org/10.1016/j.chemosphere.2020.128428>
- [4] Ghazali, N.B., Hashim, D.F., Seman, F.C., Isa, K., Ramli, K.N., Abidin, Z.Z., Mustam, S.M., Al Haek, M. (2021). Cable fault classification in ADSL copper access network using machine learning. *International Journal of Advances in Intelligent Informatics*, 7(3): 318-328. <https://doi.org/10.26555/ijain.v7i3.488>
- [5] Asmael, M., Nasir, T., Zeeshan, Q., Safaei, B., Kalaf, O., Motallebzadeh, A., Hussain, G. (2022). Prediction of properties of friction stir spot welded joints of AA7075-T651/Ti-6Al-4V alloy using machine learning algorithms. *Archives of Civil and Mechanical Engineering*, 22(2): 94. <https://doi.org/10.1007/s43452-022-00411-x>
- [6] Yehia, H.M., Allam, S. (2021). Hot pressing of Al-10 wt% Cu-10 wt% Ni/x (Al<sub>2</sub>O<sub>3</sub>-Ag) nanocomposites at different heating temperatures. *Metals and Materials International*, 27: 500-513. <https://doi.org/10.1007/s12540-020-00824-4>
- [7] Mishra, A., Vats, A. (2021). Supervised machine learning classification algorithms for detection of fracture location in dissimilar friction stir welded joints. *Frattura ed Integrità Strutturale*, 15(58): 242-253. <https://doi.org/10.3221/IGF-ESIS.58.18>
- [8] Torbati-Sarraf, H., Niverty, S., Singh, R., Barboza, D., De Andrade, V., Turaga, P., Chawla, N. (2021). Machine-learning-based algorithms for automated image segmentation techniques of transmission X-ray microscopy (TXM). *JOM*, 73(7): 2173-2184. <https://doi.org/10.1007/s11837-021-04706-x>
- [9] Karathanasopoulos, N., Pandya, K.S., Mohr, D. (2021). Self-piercing riveting process: Prediction of joint characteristics through finite element and neural network modeling. *Journal of Advanced Joining Processes*, 3: 100040. <https://doi.org/10.1016/j.jajp.2020.100040>
- [10] Aydin, F. (2021). The investigation of the effect of particle size on wear performance of AA7075/Al<sub>2</sub>O<sub>3</sub> composites using statistical analysis and different machine learning methods. *Advanced Powder Technology*, 32(2): 445-463. <https://doi.org/10.1016/j.apt.2020.12.024>
- [11] Pandya, K.S., Roth, C.C., Mohr, D. (2020). Strain rate and temperature dependent fracture of aluminum alloy 7075: Experiments and neural network modeling. *International Journal of Plasticity*, 135: 102788. <https://doi.org/10.1016/j.ijplas.2020.102788>
- [12] Li, G., Datta, S., Chattopadhyay, A., Iyyer, N., Phan, N. (2019). An online-offline prognosis model for fatigue life prediction under biaxial cyclic loading with overloads. *Fatigue & Fracture of Engineering Materials & Structures*, 42(5): 1175-1190. <https://doi.org/10.1111/ffe.12983>
- [13] Hosseini, M., Rezaei Ashtiani, H., Ghanbari, D. (2022). Properties investigation of surface nanocomposites fabricated by friction stir processing and magnetic ferrite nanoparticles. *Transactions of the Indian Institute of Metals*, 75(7): 1885-1898. <https://doi.org/10.1007/s12666-021-02468-3>
- [14] Xie, B., Fang, Q., Li, J., Liaw, P.K. (2020). Predicting the optimum compositions of high-performance Cu-Zn alloys via machine learning. *Journal of Materials Research*, 35(20): 2709-2717. <https://doi.org/10.1557/jmr.2020.258>
- [15] Marchand, D., Jain, A., Glensk, A., Curtin, W.A. (2020). Machine learning for metallurgy I. A neural-network potential for Al-Cu. *Physical Review Materials*, 4(10): 103601. <https://doi.org/10.1103/PhysRevMaterials.4.103601>
- [16] Shi, C., Liu, C., Zhu, K. (2021). Effect of friction stir processing on microstructures and mechanical properties of TIG cladding layer on AA7075. *Materials Research Express*, 8(12): 126508. <https://doi.org/10.1088/2053-1591/ac3e95>
- [17] Taşgın, Y., Ergin, R. (2022). Investigation of the effects of deformation aging applied to AA7075 aluminum alloy on mechanical and metallographic properties. *Journal of Materials Engineering and Performance*, 31(6): 4583-4603. <https://doi.org/10.1007/s11665-022-06584-z>
- [18] Hua, L., Zhang, W., Ma, H., Hu, Z. (2021). Investigation of formability, microstructures and post-forming mechanical properties of heat-treatable aluminum alloys subjected to pre-aged hardening warm forming. *International Journal of Machine Tools and Manufacture*, 169: 103799. <https://doi.org/10.1016/j.ijmactools.2021.103799>
- [19] Kazemi-Navaei, A., Jamaati, R., Aval, H.J. (2021). Asymmetric cold rolling of AA7075 alloy: The evolution of microstructure, crystallographic texture, and mechanical properties. *Materials Science and Engineering: A*, 824: 141801. <https://doi.org/10.1016/j.msea.2021.141801>
- [20] Supraja Reddy, B., Ram Gopal Reddy, B. (2021). Influence of process parameters and tool on mechanical and metallurgical properties of pure copper and aluminum alloy AA7075 dissimilar friction stir welded joints. *International Journal of Engineering Trends and Technology*, 69(9): 73-79. <https://doi.org/10.14445/22315381/IJETT-V69I9P210>
- [21] Bhattacharya, S.K., Sahara, R., Bozic, D., Ruzic, J. (2020). Data analytics approach to predict the hardness of the copper matrix composites. *arXiv preprint arXiv:2002.10649*. <https://doi.org/10.30544/567>
- [22] Abu-Okail, M., Mahmoud, T.S., Abu-Oqail, A. (2020). Improving microstructural and mechanical properties of AA2024 base metal by adding reinforced strip width of AA7075 via vertical compensation friction stir welding technique. *Journal of Failure Analysis and Prevention*, 20: 184-196. <https://doi.org/10.1007/s11668-020-00814-z>
- [23] Supraja Reddy, B., Ram Gopal Reddy, B. (2020). Experimental investigation on friction stir welding of dissimilar alloys AA7075 and pure copper: Effect of tool material and process parameters on mechanical properties. In *Advances in Materials and Manufacturing Engineering: Proceedings of ICAMME 2019*, pp. 533-540. [https://doi.org/10.1007/978-981-15-1307-7\\_60](https://doi.org/10.1007/978-981-15-1307-7_60)
- [24] Deng, Z., Yin, H., Jiang, X., Zhang, C., Zhang, K., Zhang, T., Xu, B., Zheng, Q., Qu, X. (2018). Machine learning aided study of sintered density in Cu-Al alloy. *Computational Materials Science*, 155: 48-54.

- <https://doi.org/10.1016/j.commat.2018.07.049>
- [25] Nour-Eldin, M., Elkady, O., Yehia, H.M. (2022). Timeless powder hot compaction of nickel-reinforced Al/(Al<sub>2</sub>O<sub>3</sub>-graphene nanosheet) composite for light applications using hydrazine reduction method. *Journal of Materials Engineering and Performance*, 31(8): 6545-6560. <https://doi.org/10.1007/s11665-022-06749-w>
- [26] Fang, S.F. (2018). Prediction of the hardness of Cu-Ti-Co alloy using machine learning techniques. *Key Engineering Materials*, 777: 372-376. <https://doi.org/10.4028/www.scientific.net/KEM.777.372>
- [27] Sunar, T., Tuncay, T., Özyürek, D., Gürü, M. (2020). Investigation of mechanical properties of AA7075 alloys aged by various heat treatments. *Physics of Metals and Metallography*, 121: 1440-1446. <https://doi.org/10.1134/S0031918X20140161>
- [28] Van Craen, A., Breyer, M., Pflüger, D. (2022). PLSSVM—Parallel least squares support vector machine. *Software Impacts*, 14: 100343. <https://doi.org/10.1016/j.simpa.2022.100343>
- [29] Lee, K., Son, H., Cho, K., Choi, H. (2022). Effect of interfacial bridging atoms on the strength of Al/CNT composites: Machine-learning-based prediction and experimental validation. *Journal of Materials Research and Technology*, 17: 1770-1776. <https://doi.org/10.1016/j.jmrt.2022.01.092>
- [30] Mutlu, G., Acı, Ç.İ. (2022). SVM-SMO-SGD: A hybrid-parallel support vector machine algorithm using sequential minimal optimization with stochastic gradient descent. *Parallel Computing*, 113: 102955. <https://doi.org/10.1016/j.parco.2022.102955>
- [31] Khan, M.I., Acharya, B., Chaurasiya, R.K. (2022). Automatic prediction of glycemic index category from food images using machine learning approaches. *Arabian Journal for Science and Engineering*, 47(8): 10823-10846. <https://doi.org/10.1007/s13369-022-06754-0>
- [32] Yu, Y.Y., Zhang, D., Zhang, X.M., Peng, X.B., Ding, H. (2022). Online stability boundary drifting prediction in milling process: An incremental learning approach. *Mechanical Systems and Signal Processing*, 173: 109062. <https://doi.org/10.1016/j.ymsp.2022.109062>
- [33] Yücelbaş, Ş., Yücelbaş, C. (2022). Autism spectrum disorder detection using sequential minimal optimization-support vector machine hybrid classifier according to history of jaundice and family autism in children. *Concurrency and Computation: Practice and Experience*, 34(1): e6498. <https://doi.org/10.1002/cpe.6498>
- [34] Van Craen, A., Breyer, M., Pflüger, D. (2022). PLSSVM: A (multi-) gpgpu-accelerated least squares support vector machine. In *2022 IEEE International Parallel and Distributed Processing Symposium Workshops (IPDPSW)*, Lyon, France, pp. 818-827. <https://doi.org/10.1109/IPDPSW55747.2022.00138>
- [35] Joshi, A., Sharma, S., Rao, N.V.M., Vaish, A.K. (2022). Usage of machine learning algorithm models to predict operational efficiency performance of selected banking sectors of India. *International Journal of Emerging Technology and Advanced Engineering*, 12(6): 105-114. [https://doi.org/10.46338/ijetae0622\\_14](https://doi.org/10.46338/ijetae0622_14)
- [36] Yap, C.T., Khor, K.C. (2022). Utilising sampling methods to improve the prediction on customers' buying intention. In *2022 International Conference on Decision Aid Sciences and Applications (DASA)*, Chiangrai, Thailand, pp. 352-356. <https://doi.org/10.1109/DASA54658.2022.9765293>
- [37] Wan, Y., Wang, Z., Lee, T.Y. (2021). Incorporating support vector machine with sequential minimal optimization to identify anticancer peptides. *BMC Bioinformatics*, 22(1): 286. <https://doi.org/10.1186/s12859-021-03965-4>
- [38] Jahan, S., Islam, M.R., Hasib, K.M., Naseem, U., Islam, M.S. (2021). Active learning with an adaptive classifier for inaccessible big data analysis. In *2021 International Joint Conference on Neural Networks (IJCNN)*, Shenzhen, China, pp. 1-7. <https://doi.org/10.1109/IJCNN52387.2021.9534046>
- [39] Chou, J.S., Pham, T.T.P., Ho, C.C. (2021). Metaheuristic optimized multi-level classification learning system for engineering management. *Applied Sciences*, 11(12): 5533. <https://doi.org/10.3390/app11125533>
- [40] Oliva, J.T., Rosa, J.L.G. (2021). Binary and multiclass classifiers based on multitaper spectral features for epilepsy detection. *Biomedical Signal Processing and Control*, 66: 102469. <https://doi.org/10.1016/j.bspc.2021.102469>
- [41] Gao, Z., Fang, S.C., Luo, J., Medhin, N. (2021). A kernel-free double well potential support vector machine with applications. *European Journal of Operational Research*, 290(1): 248-262. <https://doi.org/10.1016/j.ejor.2020.10.040>
- [42] Özen, A., Ganzosch, G., Völlmecke, C., Auhl, D. (2022). Characterization and Multiscale modeling of the mechanical properties for FDM-printed copper-reinforced PLA composites. *Polymers*, 14(17): 3512. <https://doi.org/10.3390/polym14173512>
- [43] Schmidt, J., Biswas, A., Vajragupta, N., Hartmaier, A. (2022). Data-oriented description of texture-dependent anisotropic material behavior. *Modelling and Simulation in Materials Science and Engineering*, 30(6): 065001. <https://doi.org/10.1088/1361-651X/ac7739>
- [44] Selvamany, P., Varadarajan, G.S., Chillu, N., Sarathi, R. (2022). Investigation of XLPE cable insulation using electrical, thermal and mechanical properties, and aging level adopting machine learning techniques. *Polymers*, 14(8): 1614. <https://doi.org/10.3390/polym14081614>
- [45] Peng, J., Xie, B., Zeng, X., Fang, Q., Liu, B., Liaw, P.K., Li, J. (2022). Vacancy dependent mechanical behaviors of high-entropy alloy. *International Journal of Mechanical Sciences*, 218: 107065. <https://doi.org/10.1016/j.ijmecsci.2022.107065>
- [46] Stoyanov, S., Bailey, C. (2022). Deep learning modelling for composite properties of PCB conductive layers. In *2022 23rd International Conference on Thermal, Mechanical and Multi-Physics Simulation and Experiments in Microelectronics and Microsystems (EuroSimE)*, St Julian, Malta, pp. 1-7. <https://doi.org/10.1109/EuroSimE54907.2022.9758885>
- [47] Sefene, E.M., Tsegaw, A.A., Mishra, A. (2022). Process parameter optimization of 6061AA friction stir welded joints using supervised machine learning regression-based algorithms. *Journal of Soft Computing in Civil Engineering*, 6(1): 127-137. <https://doi.org/10.22115/SCCE.2022.299913.1350>
- [48] Elkady, O.A., Yehia, H.M., Ibrahim, A.A., Elhabak, A.M., Elsayed, E.M., Mahdy, A.A. (2021). Direct observation of induced graphene and SiC strengthening

- in Al–Ni alloy via the hot pressing technique. *Crystals*, 11(9): 1142. <https://doi.org/10.3390/cryst11091142>
- [49] Yehia, H.M., Nyanor, P., Daoush, W.M. (2022). Characterization of Al-5Ni-0.5 Mg/x (Al<sub>2</sub>O<sub>3</sub>-GNs) nanocomposites manufactured via hot pressing technique. *Materials Characterization*, 191: 112139. <https://doi.org/10.1016/j.matchar.2022.112139>
- [50] Li, Z., Qin, L., Guo, B., Yuan, J., Zhang, Z., Li, W., Mi, J. (2022). Characterization of the convoluted 3D intermetallic phases in a recycled al alloy by synchrotron X-ray tomography and machine learning. *Acta Metallurgica Sinica*, 35(1): 115-123. <https://doi.org/10.1007/s40195-021-01312-3>
- [51] Yehia, H.M., Ali, A.I., Abd-Elhameed, E. (2023). Effect of exfoliated MoS<sub>2</sub> on the microstructure, hardness, and tribological properties of copper matrix nanocomposite fabricated via the hot pressing method. *Transactions of the Indian Institute of Metals*, 76(1): 195-204. <https://doi.org/10.21203/rs.3.rs-1409570/v1>
- [52] Zou, Y. (2021). Cold spray additive manufacturing: Microstructure evolution and bonding features. *Accounts of Materials Research*, 2(11): 1071-1081. <https://doi.org/10.1021/accountsmr.1c00138>
- [53] Thapliyal, S., Mishra, A. (2021). Machine learning classification-based approach for mechanical properties of friction stir welding of copper. *Manufacturing Letters*, 29: 52-55. <https://doi.org/10.1016/j.mfglet.2021.05.010>